DOI: 10.1002/ejoc.201300525

Systematic Modulation of Hydrogen Bond Donors in Aminoazobenzene Derivatives Provides Further Evidence for the Concerted Inversion Photoisomerization Pathway

H. M. Dhammika Bandara,[a,b] Prem N. Basa,[a] Jingjing Yan,[a] Casey E. Camire,[b] John C. MacDonald,[a] Randy K. Jackson,[b] and Shawn C. Burdette*[a]

Keywords: Diazo compounds / Photochemistry / Isomerization / Molecular devices / Hydrogen bonds

A series of aminoazobenzene derivatives structurally related to AzoAMP-1 have been prepared and characterized by using a variety of analytical techniques. AzoAMP-1 is based on 2,2′-diaminoazobenzene with *N*-methylpyridine groups. The new derivatives all contain a hydrogen bond between the aniline hydrogen atom and the azo group, as well as a separate pendant functional group that could contribute an additional hydrogen-bond acceptor to an intramolecular network. A combination of photoisomerization studies and NMR spectroscopic and X-ray crystallographic investigations suggest that AzoAMP-1 possesses a unique structure that prevents isomerization through the concerted inversion pathway, which cannot be reproduced with other types or arrangements of substituents. Only AzoAMQ, which contains a similar quinolone heterocycle in place of the pyridine group of AzoAMP-1, displayed somewhat similar photochemistry.

Introduction

Azobenzene (AB) undergoes reversible *trans*↔*cis* photoisomerization when irradiated with light (Scheme 1).[1–4] Changes in geometry and electronic structure upon isomerization enable AB to be used as a light-triggered switch. Azobenzene photoswitches have been used to tune the binding affinity of metal-chelators,[5,6] modulate the activity of biological probes,[7,8] influence catalysis,[9,10] design molecular machines,[11,12] cause structural changes in photoresponsive polymeric materials,[13,14] and alter the photochemical properties of liquid crystals,[15,16] holographic data storage devices,[17,18] and optical gratings.[19,20]

Despite the prevalence of AB derivatives in a broad spectrum of chemical applications, light is the sole input for controlling isomerization. Developing secondary switches for controlling the *trans*↔*cis* isomerization would be of considerable value for expanding the scope of possible AB applications. Computational experiments suggest that mechanical stress can induce AB isomerization;[21] in addition, electrons from the probe tip of a scanning tunneling microscope can isomerize AB molecules adsorbed on a gold surface.[22] Using structure and chemistry to control AB isomerization is more appealing; however, very few studies have examined AB structure–photochemistry relationships (SPRs) systematically.

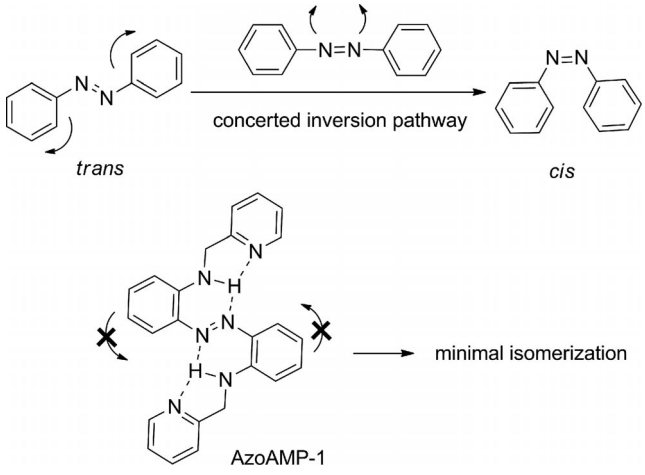

Scheme 1. Isomerization pathway in azobenzene and AzoAMP-1.

Several systems that control AB photoisomerization beyond single wavelength radiation have been reported. By introducing a redox active metal ion such as iron or cobalt coordinated onto an AB-functionalized ligand, metal oxidation state changes shift the AB absorption maximum (λ_{max}), which causes both isomers to absorb strongly at the same wavelength.[23–25] Various methods for suppressing AB *trans*→*cis* photoisomerization have also been reported. Formation of ion pairs between AB carboxylates and bulky quaternary ammonium salts block photoisomerization through steric interactions.[26] In 2-hydroxy-ABs, intramo-

[a] Department of Chemistry and Biochemistry, Worcester Polytechnic Institute,
100 Institute Road, Worcester, Massachusetts 01609-2280, USA
E-mail: scburdette@wpi.edu
Homepage: http://www.wpi.edu/academics/cbc/
[b] Department of Chemistry, University of Connecticut,
55 North Eagleville Road U-3060, Storrs, Connecticut 06269, USA

Supporting information for this article is available on the WWW under http://dx.doi.org/10.1002/ejoc.201300525.

lecular hydrogen-bonding between the azo-nitrogen atom and the hydroxyl group locks the molecule in the *trans* conformation, resulting in minimal *trans*→*cis* photoisomerization and fast thermal relaxation.[27,28] Alternately, an AB functionality may be incorporated into a metal binding ligand motif such as a crown ether[29,30] or a catechol.[31]

Previously we reported the unusual photochemistry of the substituted aminoazobenzene AzoAMP-1 (**1**; Figure 1), which exhibited minimal *trans*→*cis* photoisomerization and fast *cis*→*trans* thermal isomerization.[32] AzoAMP-1 consists of an AB core bearing two aminomethylpyridine (AMP) moieties at the arene ring *ortho* position. Computational and X-ray crystallographic data indicated intramolecular H-bonds between the anilino-hydrogen atom and azo- and pyridyl-nitrogen atoms are responsible for blocking the concerted inversion pathway in AzoAMP-1 by locking the molecule in the *trans* conformation (Scheme 1). Whereas coplanarization of the aryl groups, which is a prerequisite to isomerization by inversion, cannot occur due to the intramolecular H-bonds in AzoAMP-1 (Scheme 1), the methylated AzoAMP derivative AzoAMP-2, which lacks the ability to form intramolecular H-bonds, undergoes photoisomerization. AzoAMP-1, therefore, provides the first example of photoisomerization of AB being blocked by hydrogen-bonding amine functionalities.

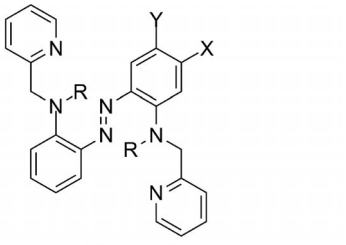

AzoAMP-1 (**1**): R = X = Y = H
AzoAMP-2 (**2**): R = CH_3, X = Y = H
AzoAMP-4 (**3**): R = CH_3, X = OH, Y = CH_3
AzoAMP-5 (**4**): R = CH_3, X = OCH_3, Y = CH_3
AzoAMP-6 (**5**): R = CH_3, X = $OCOCH_3$, Y = CH_3

Figure 1. Structure of AzoAMP compounds studied to date. AzoAMP-1 exhibits minimal photoisomerization owing to intramolecular H-bonds, whereas AzoAMP-2 photoisomerizes in a similar manner to other aminoABs. AzoAMP-4 and AzoAMP-5, with electron-donating substituents, exhibit minimal photoisomerization because of electronic effects, whereas AzoAMP-6, with the ester group, photoisomerizes in a similar manner to other aminoABs.

We also prepared the AzoAMP derivatives AzoAMP-4 and -5, which bear electron-donating hydroxy and methoxy groups, respectively, *para* to the azo moiety.[33] These AzoAMP derivatives also exhibited minimal photoiosmerization and fast thermal isomerization; however, these compounds lack any intermolecular H-bonds. When the hydroxyl group was converted into an electron-withdrawing ester group in AzoAMP-6, photoactivity was restored. Calculations showed the presence of a conical seam between S_1 and S_0 states on the *trans*-side of the S_1/S_0 crossover point in AzoAMP-4 and -5. This prevented these molecules from reaching the S_1/S_0 crossover point, which is a prerequisite for the formation of the *cis*-isomer. Further analysis showed that this conical seam is absent in AzoAMP-6, allowing it to reach the S_1/S_0 crossover point and isomerize.

Our investigation on AzoAMP compounds demonstrated that H-bonding and electronic effects can suppress AB photoactivity; however, developing reversible light-orthogonal switching mechanisms will be required to implement these concepts in practical applications. Inspired by the work on AzoAMP compounds, we investigated the extent to which H-bonding can influence AB photoactivity. To address this goal, we prepared a library of AzoAMP analogues to study SPRs by using X-ray crystallographic, UV/Vis and NMR spectroscopic analyses.

Results and Discussion

Photochemistry of Azobenzene, Aminoazobenzenes, and AzoAMP-1

The two well-separated absorption bands of *trans*-AB at ca. 320 and 450 nm correspond to π→π* and n→π* transitions, respectively.[1] Upon continuous irradiation of the π→π* transition, AB reaches a photostationary state consisting of 1:9 *trans*/*cis* isomers.[34] Because *cis*-AB is not thermodynamically stable, relaxation back to *trans*-AB occurs in the dark. Thermal relaxation of *cis*-AB has a half-life ($t_{1/2}$) of several days.[35] In contrast to AB, aminoAB derivatives containing *ortho* or *para* amine substituents exhibit different behavior. In aminoABs, the π→π* transition shifts to higher wavelengths and overlaps the n→π* transition.[36,37] Whereas, like AB, aminoABs undergo *trans*→*cis* isomerization when irradiated, thermal *cis*→*trans* isomerization occurs quickly within minutes or hours.[35] As a result, accurately determining the *trans*/*cis* ratio at the photostationary state can be difficult. Both AB and aminoABs have barely detectable emission at room temperature,[38,39] but become weakly emissive when frozen in a solid matrix at 77 K.[40]

AzoAMP-1 possesses absorption bands typical for aminoABs but exhibits remarkably different photochemistry. Upon irradiation of AzoMAP-1, only minimal photoisomerization occurs, which corresponds to a small decrease (< 5%) in integrated absorption. The thermal *cis*→*trans* isomerization occurs within seconds. X-ray crystallographic analysis shows that AzoAMP-1 adopts a completely planar structure in the solid state, despite the methylene carbon atom and aniline nitrogen atom being formally sp^3-hybridized. Intramolecular H-bonds between the aniline-hydrogen atoms and both the azo-nitrogen and pyridine-nitrogen atoms enforce the planarity. Computational experiments suggest that the H-bonding makes photoisomerization energetically unfavorable. The ^1H NMR signal for the aniline hydrogen atom of AzoAMP-1 appears significantly downfield at δ = 9.03 ppm compared with those of diaminoazobenzene (**6**; DAAB; δ = 5.20 ppm), which provides further evidence for the significance of H-bonding in the molecule.

Design and Synthesis of Aminoazobenzene Derivatives

Based on the photochemistry of AzoAMP-1, we envisioned the possibility of controlling the *trans*↔*cis* isomerization by modulating the degree of H-bonding between the aniline hydrogen atom and a dangling H-bond acceptor. The abbreviated names were derived from azobenzene (Azo); the linker between anilino nitrogen atom and the H-bond acceptor, either 2-aminomethyl (AM), 2-aminoethyl (AE), or 2-amido (A); combined with a one-letter abbreviation for the H-bond acceptor to give names corresponding to derivatives containing pyridine (AzoAMP, AzoAEP, AzoAP), quinoline (AzoAMQ), furan (AzoAMF), benzene (AzoAMB), methyl ester (AzoAME), or carboxylic acid (AzoAMC). Each compound contains the core structure of DAAB, which exhibits an intramolecular H-bond between the aniline hydrogen atom and the azo nitrogen atom on each half of the molecule.[41]

The linkers and pendant H-bond acceptors were varied to systematically change the degree of possible intramolecular H-bonding in the corresponding AB derivative (Scheme 2). Replacing the methylene linker in AzoAMP-1 with the ethylene group in AzoAEP, changes the five-membered ring formed by the H-bond to a potential six-membered ring while retaining the properties of the acceptor group. The remaining derivatives retain the five-membered ring structure but, with the exception of AzoAMQ, vary the nature of H-bond acceptor. AzoAMF contains sp^3-hybridized oxygen atoms as the H-bond acceptors, which, by virtue of the five-membered furan ring structure, orients the donor electrons at a slightly different angle to that in AzoAMP-1. Both AzoAMC and AzoAME provide H-

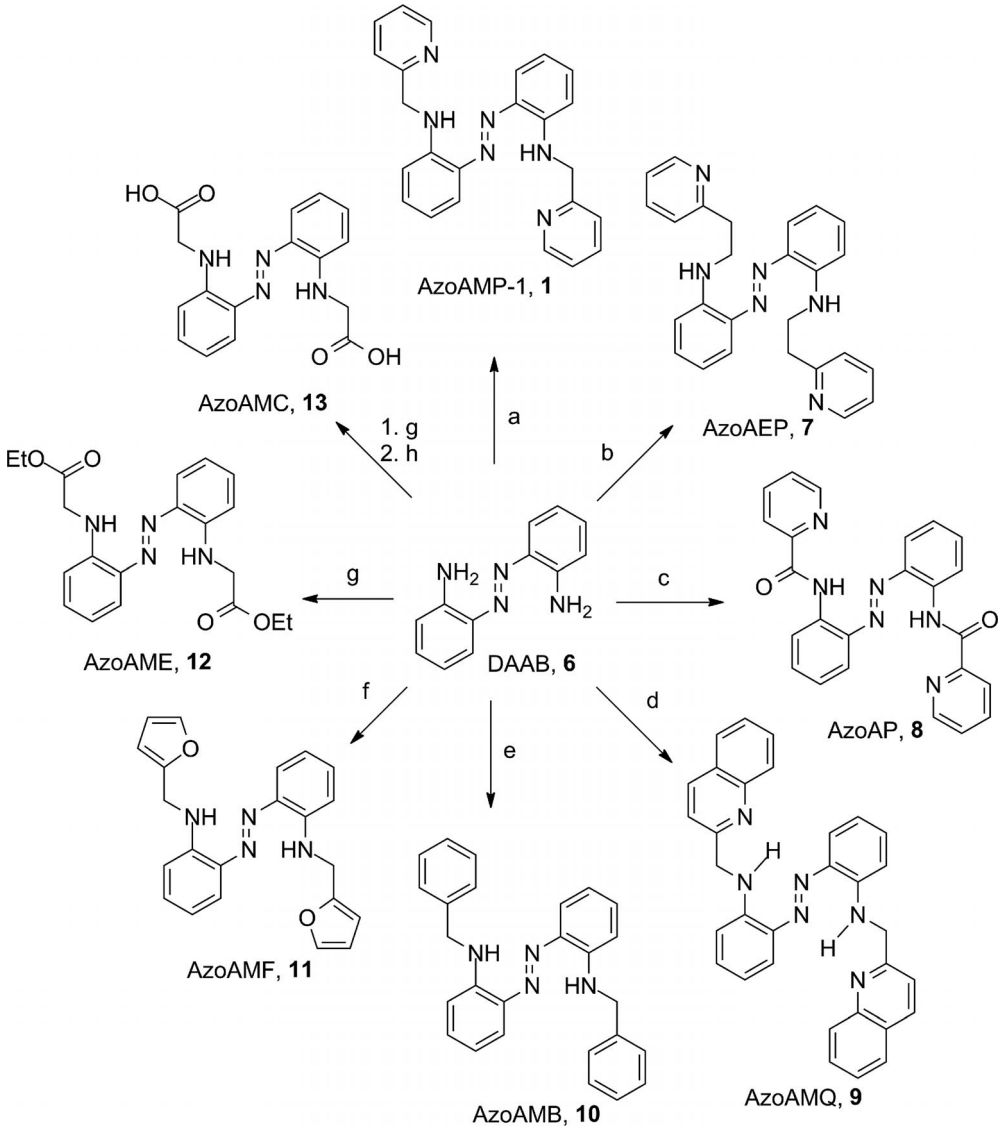

Scheme 2. Synthesis of new aminoazobenzene derivatives. *Reagents and conditions:* (a) 2-Pyridinecarbaldehyde, $NaBH(OAc)_3$, CH_2Cl_2;[32] (b) 2-vinylpyridine, AcOH, MeOH; (c) 1. picolinic acid, *N*-methylmorpholine, PyBOP, CH_2Cl_2/DMF; 2. picolinic acid chloride, K_2CO_3, THF; (d) 2-quinolinecarbaldehyde, $NaBH(OAc)_3$, CH_2Cl_2; (e) benzaldehyde, $NaBH(OAc)_3$, CH_2Cl_2; (f) 2-furalaldehyde, $NaBH(OAc)_3$, CH_2Cl_2; (g) ethyl bromoacetate, *N*,*N*-diisopropylethylamine, NaI, CH_3CN; (h) 1. 2 M NaOH, EtOH; 2. HCl.

bond acceptors through carbonyl oxygen atoms, which direct the donor electrons in a very similar manner to that in AzoAMP-1. Whereas the benzyl groups possess similar steric requirements to pyridylmethyl functionality, AzoAMB lacks the ability to form intramolecular H-bonds, like AzoAMP-1.

All AB derivatives were prepared from the DAAB scaffold (Scheme 2). AzoAMB, AzoAMF, and AzoAMQ were synthesized by reductive amination between DAAB and the appropriate aldehyde by a reaction analogous to the preparation of AzoAMP-1. AzoAEP was prepared by Michael addition with 2-vinylpyridine. AzoAP was synthesized by a two-step process using an amide coupling with picolinic acid followed by reaction with picolinic acid chloride. AzoAME was prepared by reacting DAAB with ethyl bromoacetate, and AzoAMC was prepared by the subsequent hydrolysis of ester groups. All compounds were isolated as the thermodynamically more stable *trans*-isomer, which was confirmed by ^{1}H NMR analysis.

Evidence for H-Bonding in the Solid State

Single-crystal X-ray structure determinations were carried out to investigate the extent of H-bonding present and the effect of intramolecular forces on photochemistry (Figure 2). All the AB derivatives crystallized in the thermodynamically stable *trans* conformation, typical of solid-state AB structures. The anilino nitrogen atoms in all the AB derivatives appear to be planar, despite being formally sp^3 hybridized, which enforces a planarity on the core of all the aminoAB derivatives. The orientation of the anilino hydrogen atom toward the azo nitrogen atoms and the structural planarity of the azo core suggest the presence of an intramolecular H-bond between each of the anilino hydrogen atoms and one of the azo nitrogen atoms.

The length of the NH···N=N hydrogen bond varies between 1.980 to 2.357 Å, with DAAB (2.330 Å),[41] AzoAP (2.208 Å), and AzoAEP (2.357 Å) as the only derivatives with bond lengths exceeding 2.07 Å (Table 1). The parent DAAB lacks an alkyl substituent on the aniline group, which accounts for the bond lengthening, but the behavior of AzoAEP and AzoAP appears to be more complex. Upon examination of the neighboring molecules in the crystal lattice, it is clear that the pyridyl groups of each AzoAEP compound engage in an intermolecular H-bond at 2.296(2) Å with anilino hydrogen atoms of two adjacent AzoAEP molecules. Similarly, the two anilino hydrogen atoms engage in intermolecular H-bonds with the pyridine groups of neighboring AzoAEP molecules, so each AzoAEP unit H-bonds independently to four additional AzoAEP molecules to make a hydrogen-bonded network. The intermolecular interactions can account for the longer intramolecular NH···N=N H-bond in the solid state. AzoAP lacks intermolecular H-bonding between the heteroatoms, so the longer intramolecular NH···N=N H-bond can be attributed to the presence of the amide carbonyl group.

AzoAMP-1 exhibits an apparent 2.219 Å H-bonding interaction between the dangling pyridine group and the anilino hydrogen atom. This H-bond was hypothesized to be responsible for reduced *trans*→*cis* photoisomerization.[32] AzoAMB lacks any H-bond acceptors; in addition, no interaction was observed in AzoAMF or AzoAEP, which do possess heteroatoms that could engage in a second H-bonding interaction. The oxygen atoms in the furanyl rings orient away from the azo core in AzoAMF and twist by roughly 45° with respect to the parent diaminoAB plane. Unlike in AzoAEP, for which intermolecular H-bonding can account for the lack of a heteroatom-anilino hydrogen atom interaction, AzoAMF does not engage in intermolecular H-bonds.

AzoAME (2.338 Å), AzoAMC (2.355 Å), AzoAMQ (2.305 Å), and AzoAP (2.191 Å) all appear to contain H-

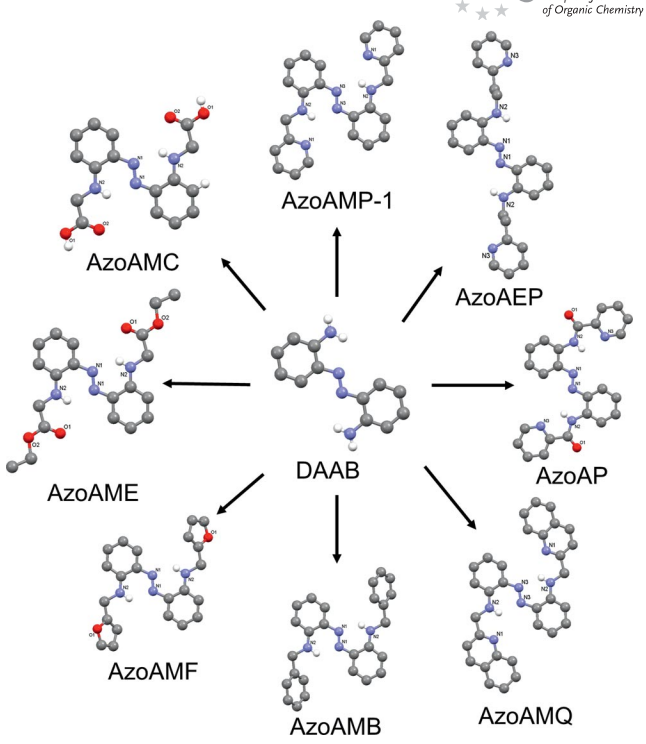

Figure 2. ORTEP diagram of aminoAB derivatives showing 50% thermal ellipsoids and selected atom labels. Hydrogen atoms on carbon atoms are omitted for clarity. The structures of AzoAMP-1[32] and DAAB[41] were previously determined.

Table 1. Hydrogen bond lengths [Å] in new aminoazobenzene derivatives.

Compound	NH···N=N	NH···X[a]
DAAB	2.330(2)	n.a.
AzoAMP-1	2.046(1)	2.219(2)
AzoAP	2.208(1)	2.191(1)
AzoAEP	2.467(2)	n.a.
AzoAMQ	2.066(6)	2.305(5)
AzoAMF	2.023(1)	n.a.
AzoAME	2.012(1)	2.338(2)
AzoAMC	2.046(2)	2.355(3)
AzoAMB	1.980(1)	n.a.

[a] n.a.: not applicable. Estimated standard deviations in the last digit(s). Atom labels are provided in Figure 2. Pendant H-bond acceptor AzoAMP-1, AzoAP, AzoAMQ: X = N; AzoAME, AzoAMC: X = O.

bonds, based on examination of the orientation of the donor group toward the anilino hydrogen atom, but only AzoAP has a H-bond length that is close to the length measured in AzoAMP-1, which suggests the interaction will be weaker in these derivatives. Whereas the NH···pyridine H-bond is shorter in AzoAP than in AzoAMP-1, NH···N=N is longer and may be more indicative of the structural changes associated with the amide group than the strength of the respective H-bonds.

Degree of H-Bonding in Solution

The anilino ^{1}H NMR signals of DAAB appear at δ = 5.02 ppm, whereas those of AzoAMP-1 appear at δ = 9.03 ppm (Table 2). The crystal structure of both DAAB and AzoAMP-1 show H-bonding between the azo group and the aniline hydrogen atom, so the additional downfield shifting of the AzoAMP-1 ^{1}H NMR signal derives from a combination of contributions from the pendant alkyl group and additional H-bonding to the pyridine nitrogen atom. In contrast to AzoAMP-1, the AzoAMB phenyl group cannot contribute an additional H-bond to the anilino hydrogen atom that appears at δ = 8.52 ppm. With the exception of AzoAMQ and AzoAP, the anilino ^{1}H NMR signal of the diaminoAB derivatives falls between 8.26–8.52 ppm, which suggests minimal H-bonding occurs with the pendent H-bond acceptors. Consistent with the structural similarity to AzoAMP-1, AzoAMQ has a nearly identical chemical shift for the anilino hydrogen atoms.

The upfield ^{1}H NMR signals for the aniline hydrogen atoms in AzoAME and AzoAMC in solution suggest a lack of a H-bond between the carbonyl oxygen atom and anilino hydrogen atom, despite the X-ray structure indicating one in the solid state. The spectrum of AzoAMC was acquired in [D_6]dimethyl sulfoxide for solubility reasons, which could disrupt H-bonding; however, the data for AzoAME was obtained in $CDCl_3$ like the other derivatives. The anilino ^{1}H NMR signal in AzoAME is also sharper than that observed in the other aminoAB compounds, so some fluctional H-bonding probably occurs. The difference between the solution-state and solid-state data in AzoAMC and AzoAME suggest that crystal packing contributes significantly to the H-bond observed in the X-ray structure.

The downfield signal (δ = 12.0 ppm) for the anilino hydrogen atoms along with the X-ray structure provides evidence that AzoAP could possess H-bonding between the pyridine nitrogen atom and the anilino hydrogen atom in both solution and the solid state. For comparison, the anilino ^{1}H NMR signal of *N*-phenyl-2-pyridinecarboxamide[42] appears at δ = 10.03 ppm,[43] 12.75 ppm in *N*-(2-benzoylphenyl)picolinamide, and 10.2 ppm for 4-(picolinoylamino)acetophenone,[44] which all contain similar structural features to AzoAP. The anilino ^{1}H NMR signal of AzoAP appears downfield closest to that of *N*-(2-benzoylphenyl)-picolinamide, which contains a H-bond accepting carbonyl oxygen in the same position as the azo group as well as the picolinamide group. When the structure lacks an H-bond acceptor, as in *N*-phenyl-2-pyridinecarboxamide, or the electron-withdrawing ketone cannot H-bond, as in 4-(picolinoylamino)acetophenone, the anilino ^{1}H NMR signal appears shifted more upfield. The combination of solution and X-ray data suggest an intramolecular H-bonding network in AzoAP that is similar to AzoAMP-1.

Photoisomerization and Thermal Relaxation in Solution

To assess photoisomerization in the aminoABs, a 3.00 mL aliquot of a 25 μM solution of each derivative in 1:1 EtOH/Et_2O was placed in a quartz cuvette and irradiated with a 1000 W light source. AzoAP experiments were conducted at 100 μM due to the weaker extinction coefficient of the derivative. Upon irradiation, a decrease in absorbance consistent with *trans*→*cis* isomerization was observed for all aminoABs (Table 2); however, the rate of thermal *cis*→*trans* isomerization precludes accurate measurement of the *trans*/*cis* isomer ratio using standard steady-state techniques for all the new compounds except AzoAP. Because the *cis*-AB isomers absorb weaker than the *trans* isomer at λ_{max}, the decrease in absorbance corresponds to disappearance of the *trans* isomer. As an indirect indicator of the degree of photoisomerization, the integrated absorption was calculated and compared with that of DAAB, AzoAP, and AzoAMP-2, which have photostationary states containing approximately 3:1 *trans*/*cis* isomer and that of AB, which reaches a 1:9 ratio.

Table 2. Photophysical properties of aminoazobenzene derivatives.

Compound	λ_{max} [nm]	ε [M^{-1} cm^{-1}]	Abs. change [%][a]	$\Phi_{trans\rightarrow cis}$	δ aniline H [ppm]	Half-life of *cis*-isomer
AB	320	22000	> 90	0.10–0.20,	n.a.	> 2 days
	450	400		0.25–0.35		
DAAB	469	11000	30	n.a.	5.20	n.a.
AzoAMP-1	490	10800	11	n.a.	9.03	< 5 s
AzoAMP-2	456	9000	35	0.19	n.a.	25 min
AzoAEP	500	13000	19	n.a.	8.29	18 s
AzoAP	410	8500	29	0.20	12.5	4 min
AzoAMQ	499	9200	20	n.a.	9.25	13 s
AzoAMB	499	15200	27	n.a.	8.52	25 s
AzoAMF	490	13200	29	n.a.	8.30	35 s
AzoAME	483	11200	28	n.a.	8.68	60 s
AzoAMC	486	11200	n.a.	n.a.	8.26	n.a.

[a] Change in integrated absorbance.

In DAAB and AzoAMB, which only contain an intramolecular H-bond between the anilino hydrogen atom and the azo group, an approximate 30% decrease in integrated absorbance was observed following irradiation. In AzoAMP-2, which has no intramolecular H-bonds, a 35% decrease in integrated absorbance was observed following irradiation. The decreased absorbance change in DAAB and AzoAMB compared with AB reflects decreased *trans*→*cis* conversion of this class of ABs, as typified by AzoAMP-2. A similar decrease in absorbance was observed in AzoAMF, AzoAME, and AzoAMC, which bear oxygen-derived H-bond acceptors. The modest, but measurable photoisomerization in these molecules provides additional proof that the dangling ligand does not contribute significantly to intramolecular H-bonds and is consistent with the NMR studies. In contrast, the integrated absorption for AzoAMQ changes by 20%, indicating slightly decreased intramolecular H-bonds in AzoAMQ compared with AzoAMP-1, which prevent photoisomerization by inhibiting the concerted inversion pathway. AzoAEP exhibits anomalous behavior. Although spectroscopic evidence suggests that minimal photoisomerization occurs, the NMR analysis does not indicate any H-bonding through the pyridine group; however, this does not preclude intermolecular phenomena like those observed in the X-ray analysis, which could prevent isomerization. AzoAEP and several structurally related compounds are the subject of an ongoing research effort involving metal complexation.

When left in the dark, the absorbance of all aminoABs except that of AzoAMC recovered completely, due to *cis*→*trans* thermal relaxation. Irradiation of AzoAMC resulted in irreversible changes in the absorption spectrum, indicating photodegradation of the compound. The rate of thermal isomerization was generally faster in AzoAMP-1 and AzoAMQ, for which the heterocyclic nitrogen atom can engage in H-bonding. Minimal photoisomerization and fast thermal isomerization in these derivatives indicate that the intramolecular hydrogen bonds inhibit the concerted inversion pathway as well as increase the thermodynamic stability of the *trans*-isomer.

AzoAP does not behave like aminoAB because the anilino lone pair can engage in resonance with the carbonyl oxygen rather than the AB ring system. The change in the nature of the substituent is also reflected in red-shifting of the absorption wavelengths, which is typical of amidoABs.[37,45,46] Upon irradiation, the integrated absorption decreases 29% and reaches an apparent photostationary state within 1 min (Figure 3). A small increase in absorbance was observed at wavelengths greater than 480 nm, as expected for ABs bearing amide substituents.[45,46] The slow AzoAP thermal *cis*→*trans* isometization allowed the photoisomerization quantum yield ($\Phi_{trans\rightarrow cis}$) to be quantified by ^{1}H NMR analysis. To determine $\Phi_{trans\rightarrow cis}$, a 3.4 mM solution of *trans*-AzoAP in $CDCl_3$ was placed in an NMR tube and the ^{1}H NMR spectrum was recorded. The NMR tube and its contents were then irradiated and the ^{1}H NMR spectrum was measured again. Irradiation caused the formation of *cis*-AzoAP, resulting in the growth of new resonances in the ^{1}H NMR spectrum. The *trans*/*cis* isomer ratio was determined from integrated peak areas of anilino hydrogen atoms, and $\Phi_{trans\rightarrow cis}$ was calculated. Irradiation converted 25% of AzoAP into the *cis*-isomer with $\Phi_{trans\rightarrow cis}$ = 20%, which is typical of azobenzenes bearing amide functionalities.[29,47] AzoAP photochemistry reflects the impact of the electronic effects of amide groups, which dominate any effect introduced by intramolecular hydrogen bonds.

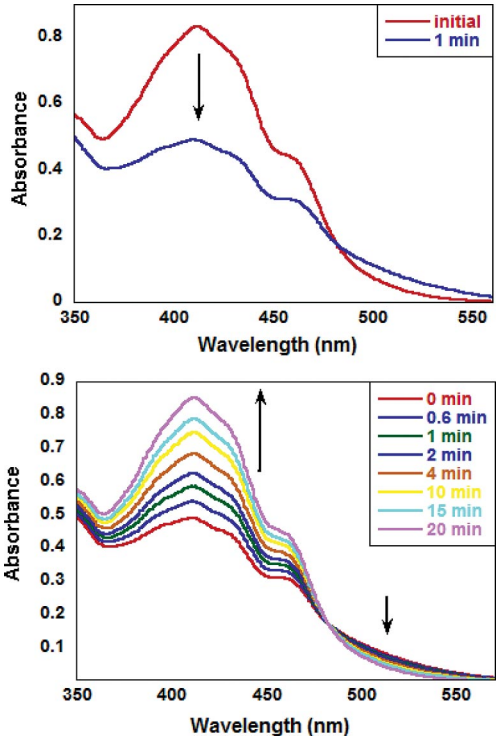

Figure 3. Absorption changes in AzoAP. Irradiation of *trans*-AzoAP leads to isomerization, with a steady state 3:1 *trans*/*cis* isomer ratio being reached after 1 min (top). In the dark, AzoAP returns to the original all-*trans* state in 20 min (bottom).

Conclusions

The photochemical properties of AminoABs differ from those of the parent AB chromophore, but both classes of molecules undergo *trans*→*cis* isomerization upon irradiation with light. Intramolecular H-bonds prevent isomerization in AzoAMP-1 by blocking the concerted inversion pathway; however, after investigating at a series of related aminoAB derivatives with differing H-bond acceptors replacing the pyridine groups it is clear that this photochemistry remains unique. Whereas ^{1}H NMR and X-ray studies provide evidence for a degree of H-bonding in solution and in the solid state, none of the intramolecular forces appear to be strong enough to block concerted inversion as efficiently as in AzoAMP-1. AzoAEP exhibits some anomalous properties that are under further investigation along with a series of related derivatives.

Introducing a secondary switch to block photoisomerization remains a long-term goal of this research. Presently,

there is no effective way to disrupt the H-bonding in AzoAMP-1 to restore *trans*→*cis* isomerization, and no means of effectively preventing the isomerization without a pendant pyridyl group. Whereas the simplicity of H-bonding provides an attractive strategy for blocking isomerization, tuning the strength of the interaction has proven to be more difficult than originally hypothesized; however, these studies support the concerted inversion mechanism of AB photoisomerization. To inhibit photoisomerization, the concerted inversion pathway must be energetically unfavorable and only the H-bonding in AzoAMP-1 can prevent the aryl group distortions that are a prerequisite to isomerization by inversion. Alternative means to toggle between a photoactive and photoinactive states in AB derivatives are being investigated by our group.

Experimental Section

General Procedures: All reagents were purchased and used without further purification. 2,2′-Diaminoazobenzene (**6**; DAAB) was prepared according to literature procedures.[48] Dichloromethane (CH_2Cl_2) and toluene were sparged with argon and dried by passage through alumina-based drying columns. All chromatography and thin-layer chromatography (TLC) were performed on silica (200–400 mesh). TLCs were developed by using EtOAc/hexanes mixtures. ^1H and ^{13}C NMR spectra were recorded with a 400 MHz NMR instrument. Chemical shifts are reported in ppm relative to tetramethylsilane (TMS). IR spectra were recorded with an FTIR instrument and samples were analyzed neat. High-resolution mass spectra were recorded in positive ion mode (+ESI).

2,2′-Bis[*N*,*N*′-(2-pyridyl)ethyl]diaminoazobenzene (AzoAEP, 7): DAAB (300 mg, 1.4 mmol) in MeOH (35 mL) was combined with acetic acid (170 μL, 3.8 mmol) and freshly distilled 2-vinylpyridine (260 μL, 3.8 mmol). The mixture was stirred at 65 °C for 12 h and allowed to cool to room temperature. After removing half of the MeOH, ice (50 g) was added and the resulting homogeneous solution was made basic (pH 10) with 1 M KOH. The product was extracted with EtOAc (3 × 20 mL), the organic layers were combined, dried with $MgSO_4$, and the solvent was removed under vacuum. Flash chromatography on silica (EtOAc/hexanes, 1:9) gave **7** (380 mg, 64%) as a dark-red solid; m.p. 152–153 °C; R_f = 0.20 (silica; EtOAc/hexanes, 1:5). ^1H NMR (400 MHz, $CDCl_3$): δ = 8.58 (d, J = 5.0 Hz, 2 H), 8.28 (s, 1 H), 7.59 (t, J = 6.8 Hz, 4 H), 7.28–7.19 (m, 5 H), 6.87 (d, J = 8.6 Hz, 2 H), 6.75 (t, J = 8.0 Hz, 2 H), 3.73 (t, J = 6.7 Hz, 4 H), 3.21 (t, J = 6.7 Hz, 4 H) ppm. ^{13}C NMR (100 MHz, $CDCl_3$): δ = 159.0, 150.4, 143.9, 137.1, 131.8, 127.5, 123.4, 116.5, 112.2, 43.0, 38.0 ppm. IR (neat): $\tilde{\nu}$ = 3323.9, 3070.2, 3006.4, 2926.5, 1595.0, 1566.4, 1504.0, 1472.5, 1433.1, 1363.6, 1318.9, 1308.1, 1287.3, 1246.9, 1210.9, 1172.9, 1144.8, 1113.8, 1095.0, 1075.7, 1042.5, 1002.5, 994.0, 880.8, 856.6, 834.0, 794.2, 768.8, 736.6 cm^{-1}. HRMS (+ESI): m/z calcd. for $C_{26}H_{26}N_6^+$ 423.2297; found 423.2279.

2,2′-Bis[*N*,*N*′-(2-picolinamide)]diaminoazobenzene (AzoAP, 8): A suspension of picolinic acid (240 mg, 2.0 mmol) in CH_2Cl_2 (7 mL) was cooled to 0 °C and *N*-methylmorpholine (220 μL, 2.0 mmol) and benzotriazol-1-yl-oxytripyrrolidinophosphonium hexafluorophosphate (PyBOP, 520 mg, 1.0 mmol) were added. The reaction mixture was warmed to room temperature and stirred for an additional 12 h. The reaction mixture was treated with a solution of DAAB (210 mg, 1.0 mmol) in DMF (5 mL) and stirred for another 12 h. The reaction mixture was diluted with EtOAc (10 mL) and washed with 2 M aqueous HCl (10 mL) and saturated aqueous NaCl (10 mL). The organic layer was dried with $MgSO_4$ and the solvent was removed. Column chromatography on silica (EtOAc/hexanes, 4:6) gave the monoamide as a red solid. The monoamide (100 mg, 0.32 mmol), picolinic acid chloride (300 mg, 2.1 mmol), and K_2CO_3 (440 mg, 3.2 mmol) were combined in THF (10 mL) and stirred at 23 °C for 24 h. The mixture was filtered, the filtrate was collected, and the solvent was removed under vacuum. The crude residue was purified by column chromatography on alumina (hexanes/EtOAc, 5:1) to give **6** (80 mg, 60%) as a light-orange solid; m.p. > 260 °C; R_f = 0.25 (alumina; EtOAc/hexanes, 1:4). ^1H NMR (400 MHz, $CDCl_3$): δ = 8.93 (t, J = 8.3 Hz, 2 H), 8.68 (s, 2 H), 8.34 (d, J = 7.8 Hz, 2 H), 8.16 (d, J = 8.9 Hz, 2 H), 7.94 (t, J = 8.2 Hz, 2 H), 7.6 (t, J = 7.8 Hz, 2 H), 7.56 (s, 2 H), 7.29 (s, 2 H) ppm. ^{13}C NMR (100 MHz, $CDCl_3$): δ = 162.2, 150.4, 148.5, 140.8, 137.8, 137.5, 133.4, 126.8, 124.0, 122.7, 120.58, 117.57 ppm. IR (neat): $\tilde{\nu}$ = 3300.2, 2920.7, 2850.9, 1682.5, 1586.3, 1568.1, 1464.7, 1448.7, 1427.2, 1311.32, 1280.7, 1259.8, 1238.5, 1155.0, 1087.2, 1018.8, 997.2, 950.6, 902.1, 869.6, 790.7, 764.3, 741.2, 700.9, 684.5 cm^{-1}. HRMS (+ESI): m/z calcd. for $C_{24}H_{19}N_6O_2^+$ 423.1569; found 423.1560.

2,2′-Bis[*N*,*N*′-(2-quinoline)methyl]diaminoazobenzene (AzoAMQ, 9): DAAB (200 mg, 0.94 mmol), 2-quinolinecarbaldehyde (320 mg, 2.0 mmol), and $NaBH(OAc)_3$ (466 mg, 2.2 mmol) were combined in CH_2Cl_2 (15 mL) and stirred at 23 °C for 24 h. Water (10 mL) was added and the organic layer was collected and dried with $MgSO_4$. Solvent was removed under vacuum and the residue was purified by flash chromatography on silica (hexanes/EtOAc, 1:9) to give **9** (260 mg, 56%) as a dark-red solid; m.p. 101–102 °C; R_f = 0.20 (silica; EtOAc/hexanes, 1:4). ^1H NMR (400 MHz, $CDCl_3$): δ = 9.25 (t, J = 5.3 Hz, 2 H), 8.16 (d, J = 8 Hz, 2 H), 8.08 (d, J = 8 Hz, 2 H), 8.00 (dd, J = 5.9, 1.8 Hz, 2 H), 7.80 (d, J = 7.8 Hz, 2 H), 7.76 (td, J = 7.0, 1.5 Hz, 2 H), 7.56 (td, J = 7.7, 1.2 Hz, 2 H), 7.4 (d, J = 8.7 Hz, 2 H), 7.27–7.25 (m, 2 H), 6.87–6.83 (m, 4 H), 4.82 (d, J = 5.16 Hz, 2 H) ppm. ^{13}C NMR (100 MHz, $CDCl_3$): δ = 158.6, 143.2, 137.5, 136.9, 131.8, 129.9, 129.2, 127.98, 127.9, 127.6, 126.5, 119.6, 116.5, 112.4, 49.5 ppm. IR (neat): $\tilde{\nu}$ = 3253.7, 3070.1, 2833.1, 1604.2, 1552.2, 1497.0, 1438.5, 1421.0, 1386.8, 1347.2, 1310.9, 1247.7, 1194.7, 1151.4, 1130.5, 1109.8, 1082.8, 1046.3, 964.3, 938.4, 811.2, 770.1, 753.43, 738.3 cm^{-1}. HRMS (+ESI): m/z calcd. for $C_{32}H_{27}N_6^+$ 495.2297; found 495.2338.

2,2′-Bis[*N*,*N*′-(2-benzyl)methyl]diaminoazobenzene (AzoAMB, 10): DAAB (100 mg, 0.47 mmol), benzaldehyde (96 μL, 0.94 mmol), and $NaBH(OAc)_3$ (250 mg, 1.2 mmol) were combined in CH_2Cl_2 (15 mL) and stirred at 23 °C for 24 h. The reaction was quenched by adding water (10 mL), the organic layer was separated, dried with $MgSO_4$, and the solvent was removed under vacuum. Flash chromatography on silica (EtOAc/hexanes, 1:19) gave **10** (140 mg, 76%) as a bright-orange solid; m.p. 133–135 °C; R_f = 0.35 (silica; EtOAc/hexanes, 1:4). ^1H NMR (400 MHz, $CDCl_3$): δ = 8.57 (s, 2 H), 7.61 (dd, J = 8.0, 1.3 Hz, 2 H), 7.41–7.30 (m, 10 H), 7.23 (t, J = 7.6 Hz, 2 H), 6.78–6.74 (m, 4 H), 4.49 (s, 4 H) ppm. ^{13}C NMR (100 MHz, $CDCl_3$): δ = 143.3, 139.0, 136.7, 131.7, 128.9, 127.9, 127.5, 127.5, 116.5, 112.4, 47.4 ppm. IR (neat): $\tilde{\nu}$ = 3234.8, 3064.0, 3034.1, 2874.9, 2839.9, 1886.4, 1680.7, 1606.8, 1558.2, 1503.5, 1458.6, 1449.2, 1419.7, 1363.1, 1327.8, 1315.1, 1303.0, 1239.4, 1221.1, 1201.2, 1152.1, 1124.8, 1082.2, 1066.0, 1043.3, 1028.2, 932.2, 908.0, 870.3, 844.3, 831.4, 778.8, 733.6, 696.4 cm^{-1}. HRMS (+ESI): m/z calcd. for $C_{26}H_{24}N_4^+$ 393.2079; found 393.2048.

2,2′-Bis[*N*,*N*′-(2-furanyl)methyl]diaminoazobenzene (AzoAMF, 11): DAAB (300 mg, 1.4 mmol), 2-furaldaldehyde (300 mg, 3.1 mmol),

and $NaBH(OAc)_3$ (750 mg, 3.5 mmol) were combined in CH_2Cl_2 (25 mL). The mixture was stirred at 23 °C for 24 h. Water (10 mL) was added and the organic layer was collected and dried with $MgSO_4$. Solvent was removed under vacuum and the residue was purified by flash chromatography on silica (hexanes/EtOAc, 1:10) to give **11** (390 mg, 74%) as an orange-red solid; m.p. 115–116 °C; R_f = 0.25 (silica; EtOAc/hexanes, 1:4). ^{1}H NMR (400 MHz, $CDCl_3$): δ = 8.29 (s, 2 H), 7.67 (d, J = 8 Hz, 2 H), 7.41 (s, 2 H), 7.28 (t, J = 8 Hz, 2 H), 6.86 (d, J = 8 Hz, 2 H), 6.82 (t, J = 8 Hz, 2 H), 6.37 (s, 2 H), 6.30 (d, J = 3.2 Hz, 2 H), 4.50 (s, 4 H) ppm. ^{13}C NMR (100 MHz, $CDCl_3$): δ = 152.5, 143.3, 142.2, 137.0, 127.1, 116.8, 112.1, 110.7, 107.2, 40.7 ppm. IR (neat): $\tilde{\nu}$ = 3237.9, 2923.0, 2851.4, 1608.2, 1559.8, 1503.9, 1469.3, 1456.7, 1424.7, 1351.7, 1330.8, 1308.5, 1252.2, 1242.4, 1227.0, 1212.6, 1186.2, 1162.6, 1141.8, 1125.4, 1081.8, 1045.2, 1009.3, 982.4, 884.4, 798.3 cm^{-1}. HRMS (+ESI): m/z calcd. for $C_{22}H_{21}N_4O_2^+$ 373.1665; found 373.1635.

2,2′-Bis[*N*,*N*′-(ethyl acetate)methyl]diaminoazobenzene (AzoAME, 12): DAAB (500 mg, 2.3 mmol), ethyl bromoacetate (770 mg, 5.0 mmol), *N*,*N*-diisopropylethylamine (750 mg, 5.8 mmol), and sodium iodide (520 mg, 3.4 mmol) were combined in CH_3CN (30 mL). The reaction mixture was heated to reflux at 70 °C for 5 h, allowed to cool to room temperature, and filtered. The residue was washed with MeCN (20 mL), the filtrates were combined and the solvent was removed under vacuum. Flash chromatography on silica (EtOAc/hexanes, 1:10) gave **12** (520 mg, 58%) as a bright-orange solid; m.p. 156–158 °C; R_f = 0.35 (silica; EtOAc/hexanes, 1:4). ^{1}H NMR (400 MHz, $CDCl_3$): δ = 8.71 (s, 1 H), 7.94 (d, J = 8.2 Hz, 2 H), 7.29 (t, J = 6.1 Hz, 2 H), 6.88 (t, J = 7.8 Hz, 2 H), 6.66 (t, J = 8.1 Hz, 2 H), 4.34 (q, J = 7.2 Hz, 4 H), 4.13 (d, J = 3.9 Hz, 4 H), 1.36 (t, J = 7.2 Hz, 6 H) ppm. ^{13}C NMR (100 MHz, $CDCl_3$): δ = 177.7, 141.8, 137.0, 132.2, 128.2, 111.7, 62.2, 45.9, 14.1 ppm. IR (neat): $\tilde{\nu}$ = 3209.0, 2989.1, 2993.8, 2838.1, 1738.7, 1609.3, 1560.8, 1504.5, 1472.1, 1439.2, 1393.2, 1374.4, 1354.4, 1333.0, 1305.8, 1110.1, 1047.7, 1017.9, 1004.0, 940.9, 883.5, 855.4, 805.5, 747.7 cm^{-1}. HRMS (+ESI): m/z calcd. for $C_{20}H_{24}N_4O_4^+$ 385.1876; found 385.1856.

2,2′-Bis[*N*,*N*′-(acetic acid)methyl]diaminoazobenzene (AzoAMC, 13): AzoAME (130 mg, 0.33 mmol) and 2 M NaOH (1.75 mL, 3.50 mmol) were combined in EtOH (10 mL) and heated to reflux for 4 h. The solution was allowed to cool to room temperature and half of the solvent was removed under vacuum. The mixture was acidified (pH 2) with 2 M HCl and the resulting precipitate was collected by filtration, washed with water (5 mL), and dried to give **13** (70 mg, 63%) as an orange solid; m.p. 171–173 °C; R_f = 0.20 (silica; EtOAc/hexanes, 1:1). ^{1}H NMR (400 MHz, [D$_6$]DMSO): δ = 12.89 (s, 2 H), 8.26 (s, 2 H), 7.83 (d, J = 7.9 Hz, 2 H), 7.28 (t, J = 7.0 Hz, 2 H), 6.77 (q, J = 7.4 Hz, 4 H), 4.09 (s, 4 H) ppm. ^{13}C NMR (100 MHz, [D$_6$]DMSO): δ = 172.8, 143.7, 136.9, 132.6, 125.6, 116.6, 111.9, 44.9 ppm. IR (neat): $\tilde{\nu}$ = 2875.8, 1721.4, 1611.6, 1565.3, 1508.2, 1471.6, 1431.3, 1408.2, 1381.7, 1335.1, 1306.1, 1251.9, 1221.0, 1158.7, 1145.6, 1094.6, 1048.3, 1003.0, 895.4, 824.2, 760.2, 734.8, 676.5 cm^{-1}. HRMS (+ESI): m/z calcd. for $C_{16}H_{17}N_4O_4^+$ 329.1250; found 329.1248.

General Spectroscopic Methods: All solutions were prepared in spectrophotometric grade solvents. Absorption spectra were recorded at 25 °C in a 1-cm path length quartz cuvette.

Photoisomerization and Thermal Relaxation: A 3.00 mL aliquot of a 1:1 EtOH/Et_2O solution was placed in a quartz cuvette and the background absorption spectrum was recorded. A 7.5 μL aliquot of an AB stock solution (10 mM) was added to obtain a 25 μM AB solution, and its spectrum was recorded. For AzoAP, a 100 μM solution was used. The solution was irradiated with a 1000 W radiation source and spectra were recorded at 30 s intervals until no further changes in absorption was observed. A 400 mL beaker containing a saturated aqueous $NaNO_3$ solution was placed in front of the light source to filter off UV radiation (< 320 nm) and prevent decomposition of the ABs. Upon completion of photoisomerization, the radiation source was turned off, and spectra were recorded at 1 min interval until thermal isomerization was complete.

Percentage Change in Absorption: The percentage change in absorption was calculated by using Equation (1).

$$\%\ abs\ change = \frac{\int_{Abs\ intial} - \int_{Abs\ final}}{\int_{Abs\ initial}} \times 100\ \% \quad (1)$$

$\int_{Abs\ initial}$ and $\int_{Abs\ final}$ are the integrated areas between 400 and 600 nm in the initial and final absorption spectra (before photoisomerization and after completion of photoisomerization), respectively.

Half-Life of the *cis*-Isomer: A 25 μL AB solution (100 μM for AzoAP) was irradiated with a 1000 W radiation source until no further change in absorption was observed. A 400 mL beaker containing a saturated aqueous $NaNO_3$ solution was placed in front of the light source to filter off UV radiation (< 320 nm) and prevent decomposition of the ABs. Upon completion of photoisomerization, the radiation source was turned off, and spectra were recorded at 1 min interval until thermal isomerization was complete. Percentage change in integrated absorption was calculated for each time interval and plotted against time, from which half-life of the *cis*-isomer (time required for percentage change in absorption to recover by 50%) was determined.

Quantum Yield of Photoisomerization: A sample of AzoAP (3.4 mg) was dissolved in $CDCl_3$ (0.60 mL) to achieve a final concentration of 13.4 mM. The solution was placed in an NMR tube and the ^{1}H NMR spectrum was recorded. The tube and its contents were irradiated for a period of 1.0 min using a 1000 W radiation source, and the ^{1}H NMR spectrum was recorded. Growth of new peaks was observed near the amide (NHCO) and aryl resonances. The [*cis*-AzoAP]/[*trans*-AzoAP] ratio was calculated by using the integrated peak areas of the NHCO resonance, from which the change in AzoAP concentration (Δ[AzoAP]) was calculated. The quantum yield of photoisomerization (Φ) of AzoAP was obtained by solving Equation (2), where N_A is the Avogadro number.

$$\phi = \frac{\Delta[AzoAP]/Irradiation\ time}{Intensity\ of\ source} \times N_A \quad (2)$$

Intensity of Source: To determine the intensity of the radiation source, a 0.60 mL aliquot of a 6 mM potassium ferrioxalate solution was placed in an NMR tube and irradiated with the 1000 W radiation source for 20 s. This resulted in the reduction of Fe^{III} oxalate to Fe^{II} oxalate. The irradiated solution was combined with ferrozine (5.2 mg, 3 equiv.), resulting in the formation of a reddish-purple solution containing [Fe(ferrozine)$_3^{2+}$], which has a molar absorption coefficient (Φ) of 27,900 cm^{-1} M^{-1} at 563 nm. A 100 μL aliquot of the resulting solution was diluted by a factor of 60, and its absorbance was measured at 563 nm. The concentration of Fe^{II} produced by the reduction of Fe^{III} oxalate is given by Equation (3).

Table 3. Crystallographic parameters for aminoazobenzene derivatives.

	AzoAEP (**7**)	AzoAP (**8**)	AzoAMQ (**9**)	AzoAMB (**10**)	AzoAMF (**11**)	AzoAME (**12**)	AzoAMC (**13**)
Formula	$C_{26}H_{26}N_6$	$C_{24}H_{18}N_6O_2$	$C_{32}H_{26}N_6{\cdot}C_{32}H_{24}N_6$	$C_{26}H_{24}N_4$	$C_{22}H_{20}N_4O_2$	$C_{20}H_{24}N_4O_4$	$C_{16}H_{16}N_4O_4{\cdot}2(C_2H_6OS)$
Formula weight	422.53	422.44	987.16	392.49	372.42	384.43	484.60
Space group	*Pbca*	$P2_1/n$	$P2_1/c$	$P2_1/c$	$C2/c$	$P2_1/c$	P
a [Å]	7.2668(7)	3.9237(4)	27.013(6)	11.3306(7)	20.6504(12)	10.111(4)	5.043(5)
b [Å]	13.6245(14)	22.575(2)	12.201(3)	12.5951(8)	12.1557(7)	11.3557(4)	11.293(5)
c [Å]	21.850(2)	11.3030(13)	7.5511(17)	7.8183(6)	7.6106(4)	9.1630(4)	11.529(5)
α [°]							60.744(5)
β [°]		94.261 (6)	98.03	108.639 (4)	104.376(4)	109.846(3)	80.664(5)
γ [°]							87.161(5)
V [Å^3]	2163.3(4)	998.41(18)	2464.3(10)	1057.23(12)	1850.59(18)	989.67(7)	564.9(7)
Z	4	2	2	2	4	2	1
$\rho_{calcd.}$ [gcm^{-3}]	1.297	1.405	1.330	1.233	1.337	1.290	1.424
Absorp. coeff. [cm^{-1}]	0.08	0.09	0.08	0.07	0.09	0.09	0.28
Temp. [K]	100	299	100	100	100	200	100
Total number of data	14383	5552	13938	8036	11172	11629	3356
Number of unique data	1869	1767	4327	1861	1633	1737	1974
Obsd. data[a]	1239	1122	1742	1200	1184	1244	1649
R [%][b]	0.045	0.021	0.106	0.028	0.031	0.033	0.034
$wR2$ [%][c]	0.106	0.082	0.366	0.092	0.102	0.134	0.110
Number of parameters	149	145	344	144	131	128	153
Max./min. peaks [e/Å]	0.13/–0.18	0.11/–0.14	0.49/–0.27	0.09/–0.13	0.11/–0.19	0.18/–0.14	0.24/–0.40

[a] Observation criterion: $I > 2\sigma(I)$. [b] $R = \Sigma||F_o| - |F_c||/\Sigma|F_o|$. [c] $wR2 = \{\Sigma[w(F_o^2 - F_c^2)^2]/\Sigma w(F_o^2)^2\}^{1/2}$.

$$[Fe(II)] = \frac{A_{563}}{\varepsilon_{563}} \times 60 \quad (3)$$

The intensity of the radiation source is given by Equation (4), where $\Phi = 1.25$.

$$Intensity\ of\ source\ (quanta\ s^{-1}\ L^{-1}) = \frac{\frac{\Delta[Fe(II)]}{Irradiation}time}{\phi} \times N_A \quad (4)$$

Collection and Reduction of X-ray Data: Crystals were covered in paratone oil on 100 μm polyimide micromounts or glued on the tip of a glass fiber and mounted on a CCD diffractometer equipped with a low temperature device. Diffraction data were collected at room temperature or at 100(2) K by using graphite monochromated Mo-K_α radiation (λ = 0.71073 Å) with the omega scan technique. Empirical absorption corrections were applied with the SADABS program.[49] The unit cells and space groups were determined with the SAINT+ program.[49] The structures were solved by direct methods and refined by full-matrix least-squares using the SHELXTL program.[49] Refinement was based on F^2 using all reflections. All non-hydrogen atoms were refined anisotropically. Hydrogen atoms on carbon atoms were all located in the difference maps and subsequently placed at idealized positions and given isotropic U values 1.2 times that of the carbon atom to which they were bonded. Hydrogen atoms bonded to oxygen atoms were located and refined with isotropic thermal parameters. Mercury 1.4.2 software was used to examine the molecular structure.[50] The crystallographic data and refinement parameters are shown in Table 3, selected hydrogen bond lengths are shown in Table 2 and the 50% thermal ellipsoid plots are shown in Figure 2.

CCDC-933539, -933540, -933541, -933542, -933543, -933544, and -933545 contain the supplementary crystallographic data for this paper. These data can be obtained free of charge from The Cambridge Crystallographic Data Centre via www.ccdc.cam.ac.uk/data_request/cif.

Supporting Information (see footnote on the first page of this article): Figures S1–S11 showing the photoisomerization and thermal relaxation of AzoAMB, AzoAEP, AzoAMF, AzoAME, AzoAMQ. ^{1}H and ^{13}C NMR spectra for all new compounds synthesized. Complete tables of X-ray data and fully labeled ORTEP diagrams.

Acknowledgments

The work was funded by Worcester Polytechnic Institute. The authors thank Professor Jim Dittami for insightful discussions.

[1] H. M. D. Bandara, S. C. Burdette, *Chem. Soc. Rev.* **2012**, *41*, 1809.
[2] G. Hartley, *Nature* **1937**, *140*, 281.
[3] E. Fischer, *J. Am. Chem. Soc.* **1960**, *82*, 3249.
[4] D. Gegiou, K. Muszkat, E. Fischer, *J. Am. Chem. Soc.* **1968**, *90*, 3907.
[5] S. Shinkai, T. Minami, Y. Kusano, O. Manabe, *J. Am. Chem. Soc.* **1983**, *105*, 1851.
[6] E. Luboch, E. Wagner-Wysiecka, Z. Poleska-Muchlado, V. C. Kravtsov, *Tetrahedron* **2005**, *61*, 10738.
[7] M. Banghart, K. Borges, E. Isacoff, D. Trauner, R. H. Kramer, *Nature Neurosci.* **2004**, *7*, 1381.
[8] M. R. Banghart, A. Mourot, D. L. Fortin, J. Z. Yao, R. H. Kramer, D. Trauner, *Angew. Chem.* **2009**, *121*, 9261; *Angew. Chem. Int. Ed.* **2009**, *48*, 9097.
[9] W. S. Lee, A. Ueno, *Macromol. Rapid Commun.* **2001**, *22*, 448.
[10] M. Zaremba, V. Siksnys, *Proc. Natl. Acad. Sci. USA* **2010**, *107*, 1259.
[11] Y. Norikane, N. Tamaoki, *Org. Lett.* **2004**, *6*, 2595.
[12] T. Muraoka, K. Kinbara, T. Aida, *Nature* **2006**, *440*, 512.
[13] H. Koshima, N. Ojima, H. Uchimoto, *J. Am. Chem. Soc.* **2009**, *131*, 6890.
[14] M. Yamada, M. Kondo, R. Miyasato, Y. Naka, J. Mamiya, M. Kinoshita, A. Shishido, Y. Yu, C. J. Barrett, T. Ikeda, *J. Mater. Chem.* **2009**, *19*, 60.
[15] T. J. White, R. L. Bricker, L. V. Natarajan, N. V. Tabiryan, L. Green, Q. Li, T. J. Bunning, *Adv. Funct. Mater.* **2009**, *19*, 3484.

[16] O. Tsutsumi, K. Yamamoto, K. Ohta, K. Fujisawa, K. Uno, T. Hashishin, C. Yogi, K. Kojima, *Mol. Cryst. Liq. Cryst.* **2011**, *550*, 105.
[17] A. Shishido, *Polym. J.* **2010**, *42*, 525.
[18] H. Audorff, R. Walker, L. Kador, H. W. Schmidt, *Chem. Eur. J.* **2011**, *17*, 12722.
[19] R. M. Parker, J. C. Gates, H. L. Rogers, P. G. R. Smith, M. C. Grossel, *J. Mater. Chem.* **2010**, *20*, 9118.
[20] L. De Sio, S. Serak, N. Tabiryan, C. Umeton, *J. Mater. Chem.* **2011**, *21*, 6811.
[21] R. Turanský, M. Konôpka, N. L. Doltsinis, I. Štich, D. Marx, *Phys. Chem. Chem. Phys.* **2010**, *12*, 13922.
[22] J. Henzl, M. Mehlhorn, H. Gawronski, K. H. Rieder, K. Morgenstern, *Angew. Chem.* **2006**, *118*, 617; *Angew. Chem. Int. Ed.* **2006**, *45*, 603.
[23] K. Yamaguchi, S. Kume, K. Namiki, M. Murata, N. Tamai, H. Nishihara, *Inorg. Chem.* **2005**, *44*, 9056.
[24] S. Kume, M. Kurihara, H. Nishihara, *Chem. Commun.* **2001**, 1656.
[25] M. Horie, T. Sakano, K. Osakada, H. Nakao, *Organometallics* **2004**, *23*, 18.
[26] O. Ohtani, T. Furukawa, R. Sasai, E. Hayashi, T. Shichi, T. Yui, K. Takagi, *J. Mater. Chem.* **2004**, *14*, 196.
[27] W. R. Brode, J. H. Gould, G. M. Wyman, *J. Am. Chem. Soc.* **1952**, *74*, 4641.
[28] M. Emond, T. Le Saux, S. Maurin, J. B. Baudin, R. Plasson, L. Jullien, *Chem. Eur. J.* **2010**, *16*, 8822.
[29] S. Shinkai, T. Nakaji, Y. Nishida, T. Ogawa, O. Manabe, *J. Am. Chem. Soc.* **1980**, *102*, 5860.
[30] A. Momotake, T. Arai, *Tetrahedron Lett.* **2003**, *44*, 7277.
[31] M. Yamamura, Y. Okazaki, T. Nabeshima, *Chem. Commun.* **2012**, *48*, 5724–5726.
[32] H. M. D. Bandara, T. R. Friss, M. M. Enriquez, W. Isley, C. Incarvito, H. A. Frank, J. Gascon, S. C. Burdette, *J. Org. Chem.* **2010**, *75*, 4817.
[33] H. M. D. Bandara, S. Cawley, J. A. Gascon, S. C. Burdette, *Eur. J. Org. Chem.* **2011**, 2916.
[34] P. Bortolus, S. Monti, *J. Phys. Chem.* **1979**, *83*, 648.
[35] G. S. Hartley, *J. Chem. Soc.* **1938**, 633.
[36] G. Cilento, E. Miller, J. Miller, *J. Am. Chem. Soc.* **1956**, *78*, 1718.
[37] A. A. Blevins, G. Blanchard, *J. Phys. Chem. B* **2004**, *108*, 4962.
[38] J. Azuma, A. Shishido, T. Ikeda, N. Tamai, *Mol. Cryst. Liq. Cryst.* **1998**, *314*, 83.
[39] T. Fujino, S. Y. Arzhantsev, T. Tahara, *J. Phys. Chem. A* **2001**, *105*, 8123.
[40] M. Nepraš, S. Luňák, R. Hrdina, J. Fabian, *Chem. Phys. Lett.* **1989**, *159*, 366.
[41] D. S. Bohle, K. Dorans, J. Fotie, *Acta Crystallogr. Sect. E: Struct. Rep. Online* **2007**, *63*, 889.
[42] P. Hermange, A. T. Lindhardt, R. H. Taaning, K. Bjerglund, D. Lupp, T. Skrydstrup, *J. Am. Chem. Soc.* **2011**, *133*, 6061.
[43] Y. Xie, Y. Yang, L. Huang, X. Zhang, Y. Zhang, *Org. Lett.* **2012**, *14*, 1238.
[44] H. Ueki, T. K. Ellis, C. H. Martin, V. A. Soloshonok, *Eur. J. Org. Chem.* **2003**, 1954.
[45] A. Airinei, E. Rusu, V. Barboiu, *J. Braz. Chem. Soc.* **2010**, *21*, 489.
[46] I. K. Lednev, T. Q. Ye, L. C. Abbott, R. E. Hester, J. N. Moore, *J. Phys. Chem. A* **1998**, *102*, 9161.
[47] H. Rau, *J. Photochem.* **1984**, *26*, 221.
[48] G. Crank, M. Makin, *Aust. J. Chem.* **1984**, *37*, 845.
[49] *Bruker SAINT*, v. 6.14 and *SHELXTL* for WinNT/2003, v. 6.14, Bruker AXS Inc., Madison, WI, **1999**.
[50] *CCDC Mercury*, v. 1.4.2, Cambridge, U. K., **2009**.

Received: April 11, 2013
Published Online: June 21, 2013

